Optoelectronic device based on Rare Earths electroluminescence

Juan Luis Frieiro Castro
Oriol Blázquez and Sergi Hernández
MIND–IN²UB, Department of Engineering: Electronics, Universitat de Barcelona, Marti i Franque's 1, E-08028 Barcelona, Spain

***Abstract*—In this Master Thesis, the fabrication and the structural, optical and electrical properties of Al/rare earth (RE)/Al/SiO_2 and RE/SiO_2 nanomultilayers have been studied. The nanomultilayers were deposited by means of e-beam evaporation on top of *p*-type Si substrates. Two different RE species were considered: Tb^{3+} and Eu^{3+} ions, as they exhibit a narrow and strong emission in the green and red spectral ranges, respectively. The main goal of the present work is achieving optical activation of those rare earth elements, and thus obtaining light emission from their intra-4f and 5d-to-4f shell transitions. Optical characterization indicates that optically active RE^{3+} ions had been successfully fabricated. The electrical and electroluminescence analysis yielded promising results to include this material in future applications of illumination and integrated emitting devices for optoelectronics.**

***Index Terms*—Nanostructured materials: rare earth ions, electron-beam evaporation, terbium, europium, luminescence, nanomultilayers, delta doping.**

I. Introduction

LIGHT EMITTING DIODES (LEDs) are junctions of p-n doped semiconductors that emit light when electrically activated. The first LEDs were studied and produced in the 1950s, but their emission was only in the spectral range from the green to the infrared. It was at the beginning of the 1990s that the first efficient blue LED was demonstrated, allowing the development of a new source of white light. They yield a 50% wallplug efficiency in the form of visible light from the electrical energy they receive, meaning a huge increase in efficiency compared to incandescent light bulbs and fluorescent tubes employed until now (4% and 18% respectively). Due to their electrical and optical properties, they are employed as indicator devices and in illumination systems, as well as in novel photonics applications [1], [2].

The invention of LEDs has opened the door for the field of optoelectronics, as the use of semiconductors allows scaling these light sources to the sizes of microelectronic devices employed today. Optoelectronic devices are designed to employ light in combination with (or instead of) electric currents, which introduces many advantages: separation of electronic devices (thus enabling the optimization of the chip layout), reduction of electromagnetic interference, cable length and cable weight, sustenance of precise signal timing, reduction of interconnect densities and energy saving (thanks to lower heat loses) [3], [4].

These new devices need to be able to operate in concert with current electronic devices based on silicon technology, which requires of Si-based light collectors, transducers between electric and optical signals, light waveguides, and light emitters. For the latter, semiconductor materials doped with rare earth (RE) ions have been widely studied in the last two decades due to their narrow and intense luminescence, as a potential alternative for more efficient devices than LEDs [5]–[7].

Rare earth elements have their 4*f* electronic shell partially filled and when they are optically active, they usually have an oxidation state +3 due to the loss of one 4*f* electron and the two 6*s* electrons. These elements have luminescent properties resulting from the intra-4*f* transitions (not very dependent of the matrix) or 5*d*-to-4*f* (sensitive to the matrix). [8]

Erbium has been studied as dopant of different films like silica (SiO_2), yielding emissions in the infrared part of the spectra (1535 nm) when ions are in the +3 oxidation state, which makes it very useful for optical fiber telecommunication systems [9], [10]. Other RE have been researched for their emission in the visible range, such as Ce^{3+} [8], Tb^{3+} [11] and Eu^{3+} [12]; in the blue (460nm), green (543 nm) and red (615 nm) regions of the visible spectrum respectively. In Fig. 1, the electronic levels, energies and transitions for two RE species (Tb^{3+} and Eu^{3+} ions employed in this project) are presented. [13], [14].

Fabrication of these materials has been exploited through many different techniques, such as plasma-enhanced chemical vapor deposition [11], ion implantation [15], liquid source

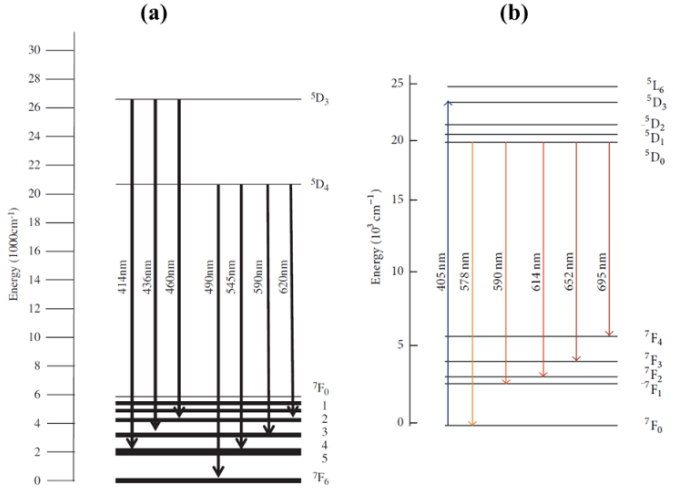

***Fig. 1.** Electronic transitions of (a) Tb^{3+} [13] and (b) Eu^{3+} [14] ions.*

chemical vapor deposition [16], magnetron sputtering [17] and sol-gel [18]. Some other techniques have also been attempted, but are less commonly employed, like atomic layer deposition [19].

Following the approach to new RE light emitters, in this Master Thesis it is described the fabrication and characterization of nanomultilayered (NML) structures composed of SiO_2, Al and Tb^{3+} or Eu^{3+} ions, by means of electron-beam evaporation (EBE). Prior to this work, different combinations of these layers (considering only Tb^{3+}) have been tried in the group to find the best layer configuration that exhibits stronger emission [20]. The optical properties of the chosen configuration were studied by photoluminescence (PL) in samples annealed at different temperatures [21].

The films employed in this Master Thesis were also deposited by using EBE, considering for Tb^{3+} the optimum nanomultilayered structure as Al/RE/Al/SiO_2, on top of a *p*-type Si substrate. The films used for the structural and optical characterization exhibit 15×Al/RE/Al/SiO_2, ending on a SiO_2 layer that serves as protection. For the electrical characterization, 5×Al/RE/Al/SiO_2 were fabricated, also on a *p*-type Si substrate, adding a full area bottom electrode of Al and top contact of indium tin oxide (ITO). The ITO contact also allows for electro-optical characterization as it is a transparent conducting oxide (TCO). In the case of Eu^{3+}, RE/SiO_2 structures were considered with 15 stacks deposited on top of a *p*-type Si substrate and ending with a SiO_2 protective layer, for optical and structural characterization.

The average composition of the nanomultilayers was assessed by using X-ray photoelectron spectroscopy (XPS). Different techniques were employed to determine the optical properties of the RE-films, using PL and cathodoluminescence (CL). The electrical properties were studied through the different *I*(*V*) curves obtained. Finally, the electroluminescence (EL) of the NMLs was also measured in the accumulation regime. The results suggest the possibility of employing EBE for fabrication of RE-doped materials that can be introduced into devices for optoelectronic applications in the future.

II. Experimental Details

The following will describe the different techniques, equipment and parameters employed in the fabrication of the samples and their characterization.

A. Fabrication

Previously to this Master Thesis project, different combinations in nanomultilayer structures were tested for SiO_2, Al and Tb or Eu, in order to achieve the optimal for the optical activation of the RE^{3+} ions [20], [21]. All test samples and the ones here employed were fabricated by electron-beam evaporation. This technique employs a high vacuum chamber in which a beam of high energy electrons impinges on a target of the material to be evaporated. The electrons transfer their energy as they travel through the target, heating the material to its evaporation (or sublimation). Deposition of the evaporated material takes place on top of the *p*-type Si substrate situated at the top of the chamber. Before been introduced into the chamber, the substrates were cleaned with acetone, isopropyl alcohol, ethanol, and de-ionized water, and agitated ultrasonically during each process.

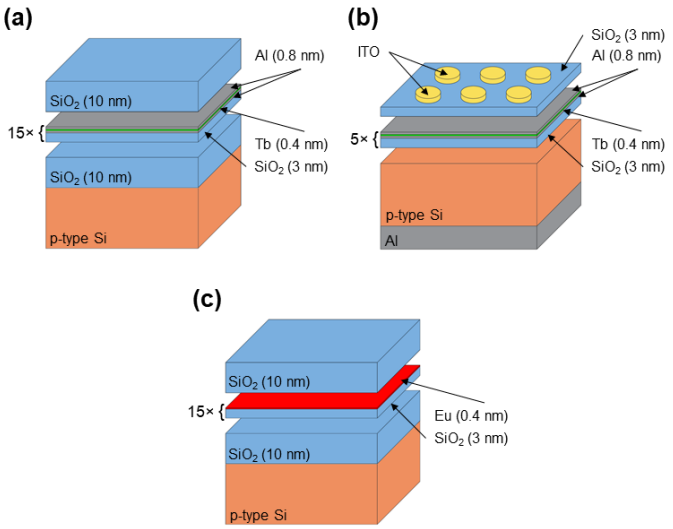

Fig. 2. *Sketch of the deposited structures:* ***(a)*** *for structural and optical characterization of* Tb^{3+}, ***(b)*** *for electrical and electro-optical characterization of* Tb^{3+}, *and* ***(c)*** *for structural and optical characterization of* Eu^{3+}.

The equipment employed in this project is a PFEIFFER VACUUM Classic 500 chamber with a Ferrotec GENIUS electron-beam controller and a Ferrotec CARRERA high-voltage power supply. The base pressure in the chamber was 1.6×10^{-6} mbar and the temperature of the substrate was kept at 100 °C. Acceleration voltages were 6 kV for SiO_2 and 10 kV for Al, with deposition rates of 1.0 Å/s and 0.2 Å/s, respectively. In the case of RE, this acceleration voltages were 6 kV and 4.5 kV for Tb and Eu, respectively; both with a deposition rate of 0.2 Å/s. Nominal thickness of the layers was the same for all the samples: 0.8 nm for Al, 0.4 nm for the RE and 3 nm for the SiO_2.

A first sample prepared for Tb^{3+} was composed of 15 stacks of Al/Tb/Al/SiO_2, deposited for structural and optical characterization, with two 10 nm layers of SiO_2 before and after them to prevent any atomic diffusion from or to the nanomultilayers [see Fig. 2(a)]. Thermal annealing was done at 1100 °C in N_2 atmosphere for 1 hour. A second sample was prepared with 5 stacks of Al/Tb/Al/SiO_2 annealed at 1100 °C in N_2 atmosphere for 1 hour. After annealing, the indium tin oxide (ITO) electrodes required for electrical and electro-optical characterization were deposited using a shadow mask, with circular shape with a radius of 200 µm, and subsequently annealed at 600 °C in N_2 atmosphere for 1 hour. Finally, a full area Al metallization was performed on the backside of the Si substrate for defining the bottom contact [see Fig. 2(b)].

For the case of Eu^{3+} only one sample was prepared, for optical and structural characterization and composed of 15 stacks of Eu/SiO_2 [see Fig. 2(c)] in between two 10 nm protective layers of SiO_2, and annealed at temperatures of 500, 700, 900 and 1100 °C in N_2 atmosphere for 1 hour.

All these stacks are employed to achieve delta doping systems of RE in an Al/SiO_2 or SiO_2 matrix, allowing to obtain nanometric separation between the RE ions in the perpendicular

direction to the deposition axis, reducing their clustering.

B. Structural characterization

To determine the compounds present at each layer, X-ray Photoelectron Spectroscopy (XPS) was used. X-rays impinging on a material excite photoelectrons which are emitted from the surface. The binding energy of these photoelectrons can be calculated from their kinetic energy, determining the different energy levels of the elements present in the sample. These energies are shifted when the corresponding element forms bonds. This information can be employed to determine the different compounds existing. In this project a PHI 5500 Multitechnique System was employed for these measurements.

C. Optical characterization

The purpose of this project is to achieve optical activation of the rare earth present in the structure. To find out if that was the case, two different methods were employed.

Photoluminescence (PL) employs light to excite a material. Deexcitation is done through the emission of photons that are recorded. Since electronic transitions are limited between levels, each element would yield a characteristic emission spectrum, and the impinging light also needs to be of a specific wavelength that corresponds to possible electronic transitions that can be absorbed. Measurements with an excitation line of λ = 325 nm were performed on a Horiba Jobin Yvon LabRAM HR with a HeCd laser. Measurements with a λ = 488 nm excitation line were done with an Ar^+ laser and the spectra were acquired with a Hamamatsu GaAs R928 PMT, which has a sensitivity from 300 nm to 850 nm, coupled to a monochromator in a lock-in configuration.

Cathodoluminescence (CL) was also utilized in this project. Its fundamentals are close to the case of PL, but in this case the excitation of the material is done employing a focused electron-beam. The equipment employed for this measurement was a JEOL JSM-7100F, with the electron-beam working at 80 μA and an acceleration voltage of 2 keV.

D. Electrical and electroluminescent characterization

Electrical characterization of the samples was done by 2 contact measurements with an Agilent B1500 semiconductor device analyzer and a Cascade Microtech Summit 11000 probe station with a thermal chuck. The devices were electrically isolated by setting them inside a Faraday cage, and the contact tips are made of Au. The back-contact was grounded through the chuck, whereas the top ITO-contact was swept from -15 V to 15 V with the tip, with steps of 50 mVs^{-1}.

Light emission from the sample obtained through electroluminescence (EL) measurements (emission of light from elements electronic deexcitation by applying an electric current for exciting), was collected with a Seiwa 888 L microscope. Integrated emission was recorded using the same GaAs PMT as was employed in PL measurements. The emission spectrum was captured by means of Princeton Instruments LN-cooled charge-coupled device via a 1/4m Oriel monochromator.

III. Results

A. Structural characterization

In a previous study done in the group (see Ref. 21), XPS measurements at different depths allowed to determine the composition and the effect of the presence of Al atoms surrounding the Tb ions, by sputtering the surface with Ar^+ ions. Measurements were performed on a structure fabricated following the same steps previously described for the 15 stacks structure [see Fig. 2(a)], as well as a similar sample that did not contain Al.

The sample with no Al showed stoichiometric SiO_2, with no extra oxygen added to the Tb layers. The addition of Al to the sample showed an excess of oxygen. Due to the fact that both Al and Tb layers are mixed, this oxygen excess is most probably bound to Al forming alumina (Al_2O_3) with all the Al atoms oxidized, and the remaining oxygen atoms are forming Tb_2O_3 (Tb ions are less reactive than Al ones). In this case, a 45% of the Tb atoms is estimated to be forming this oxide. It is concluded then that the addition of Al helps in the oxidation of Tb ions, which also modifies their emission properties (see Ref. 21 for more information regarding this issue).

The composition of the Eu/SiO_2 NML system was studied in this Master Thesis. Figure 3 displays the photoemission spectra of the different elements present in the layers: O, Si and Eu, for a sample annealed at 1100 °C. Characteristic peaks (marked in the graphs) were fitted using pseudo-Voigh functions and applying a baseline (not displayed in the graphs). Figure 3(a) shows the peak corresponding to O 1s bonding, displaced from its usual position (531 eV) due to the charging of the sample during the experiment. In Fig. 3(b), the peak shown is characteristic of the Si 2p bonding, also displaced (usual binding energy is 103 eV). Last, in Fig. 3(c) the peaks shown correspond to Eu^{2+}. Two additional peaks appear to the left of the main ones, related to the presence of some Eu^{3+} ions. The annealing of the sample yields a loss of its +3 oxidation state, as it would be later evidenced by PL measurements. Even if the oxidation state is different from that desired in the case of Eu, the amount of this element is still accurate. It was found that the

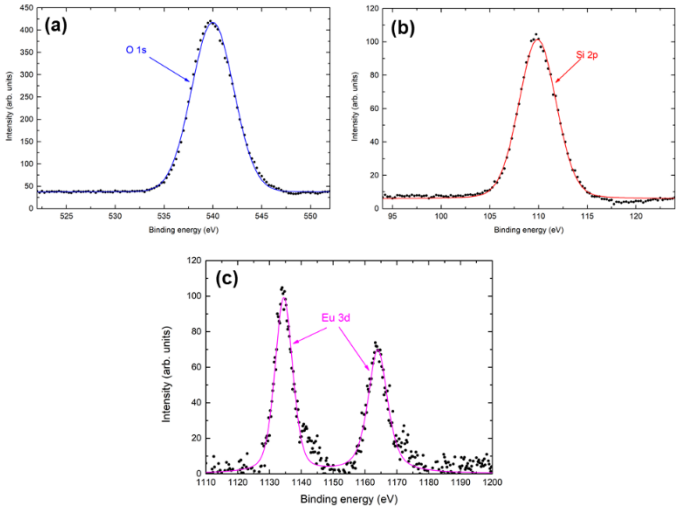

Fig. 3. *XPS peaks of the NML sample of Eu/SiO_2 for the binding energies of the bonds: (a) O 1s, (b) Si 2p and (c) Eu 3d.*

layers closer to the surface contained a larger quantity of Eu atoms in the +3 oxidation state, probably because contact with air during the thermal treatment maintained the oxidation state. Evaluation of the areas of each element gives a compositional study of the layers. As shown in Table I, the composition for each element is 64 % of O, 34 % of Si and 2 % of Eu.

TABLE I

XPS binding energies, integrated areas under the curves, and evaluated atomic compositions of the top Eu/SiO_2 NMLs.

	O 1s	Si 2p	Eu 3d
Binding energy (eV)	540.0	110.0	1134.7
			1164.4
Integrated area (arb. units)	51.97	28.28	1.29
Atomic content (%)	64	34	2

The atomic concentrations here obtained are consistent with the deposition of Si-rich SiO_2 layers doped with Eu^{2+} ions that are forming EuO. Although Eu-Si bonds and ternary bonds cannot be discarded, the fast oxidation of Eu suggests that the above mentioned is the most probable case. If Eu^{3+} ions were found, oxides would have been of the Eu_2O_3 form. Additional studies at different annealing temperatures should confirm that this kind of oxides can also be obtained, as suggested later by PL measurements.

B. Optical characterization

Optical emission of the Al/Tb/Al/SiO_2 structure was first characterized by means of PL. Two different excitation lines were employed: one of λ = 325 nm and another of λ = 488 nm (see Fig. 4). The spectrum acquired with the 325-nm line shows peaks at 489, 542, 584 and 621 nm. In the case of using the 488-nm line, the same emissions were detected but at slight different positions (542, 586 and 623 nm, respectively), except for the one at 489 nm, that cannot be observed because it is too close to the excitation wavelength. These emission bands are consequence of the electronic radiative transitions to the intra-4*f* levels as $^5D_4 \rightarrow {}^7F_J$ (J = 6, 5, 4 and 3, respectively).

Similar emission as for PL was obtained when performing CL measurements, exciting the sample with an electron-beam of 2 keV of energy. Figure 4 shows the emission spectrum collected with the characteristic peaks of Tb^{3+} at 489, 544, 587 and 624 nm. These emission bands correspond with the transitions $^5D_4 \rightarrow {}^7F_J$ (J = 6, 5, 4, 3; respectively) as previously described. Blue emission bands also appear in the CL spectrum, corresponding to $^5D_3 \rightarrow {}^7F_J$ (J =5, 4) transitions, with peaks at 415 and 437 nm. The emission with the highest intensity (544 nm) corresponds to the green visible range, while other features are located in the blue, yellow and red regions of the spectrum. All these results are in good agreement with other works found in the literature (see Ref. 22).

The presence of all the different emission bands is more visible in the case of CL as excitation takes place more often and thus the $^5D_4 \rightarrow {}^7F_5$ transition is not able to perform most of the deexcitation as in the case of PL. Difference in the intensity of emission of each band can also be seen when comparing both PL excitations, due to the fact that the spectrum acquired with

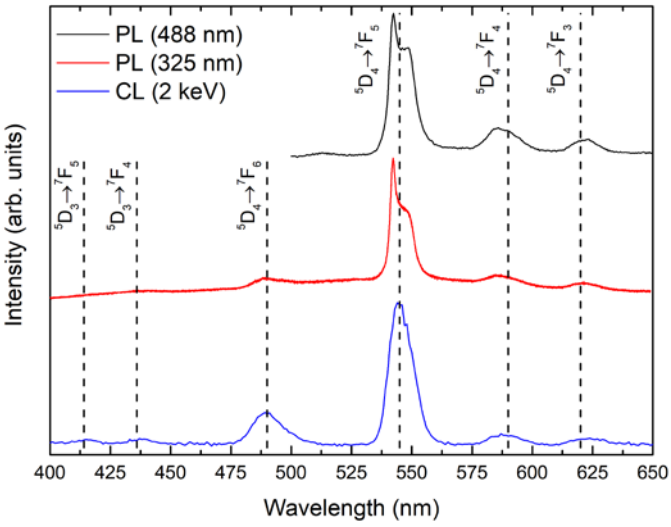

Fig. 4. *Normalized PL and CL measurements of the Al/Tb/Al/SiO_2 structure.*

the 488-nm lines is under resonant excitation (Tb^{3+} are directly excited), whereas the one acquired using the 325-nm line is excited by transference of energy from the matrix that absorbs the light. The presence of a double peak at the $^5D_4 \rightarrow {}^7F_5$ transition can be explained by the Stark effect: a splitting of the spectral lines is produced when an external electric field is applied; in this case by the matrix [8].

PL measurements were also performed for the samples containing Eu with the 325-nm. Figure 5 exhibits a comparison of the spectra of samples annealed at different temperatures. Peaks of Eu^{3+} were found at 579, 591, 615 and 650 nm (measured for the 700 °C annealing), that are characteristic of the $^5D_0 \rightarrow {}^7F_J$ (J = 0, 1, 2, 3, respectively) electronic transitions. The as-deposit sample shows a large amount of background emission, which is reduced by thermal annealing in the rest of the samples. Annealing at 500 °C maintains the emission of Eu^{3+} ions as the as-deposit sample, while 700 °C and 900 °C enhances it. When applying 1100 °C for annealing, the Eu^{3+} emission is completely quenched, as well as most of the background. Annealing at 700 °C yields the optimum emission: the lowest background signal while increasing that of the Eu^{3+}

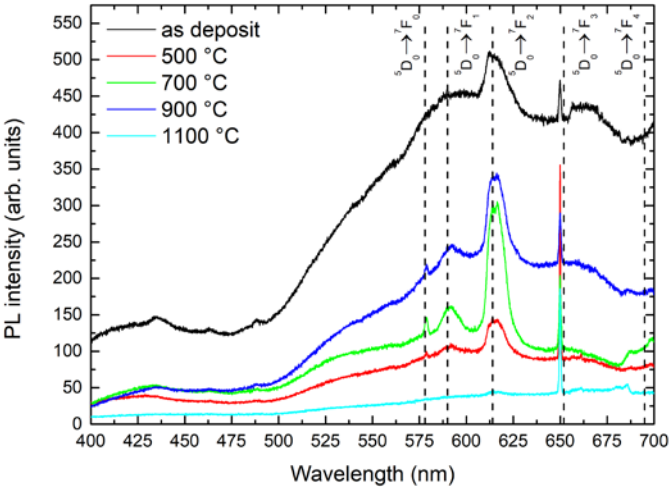

Fig. 5. *PL intensity of 15×Eu/SiO2 with different temperatures of thermal annealing.*

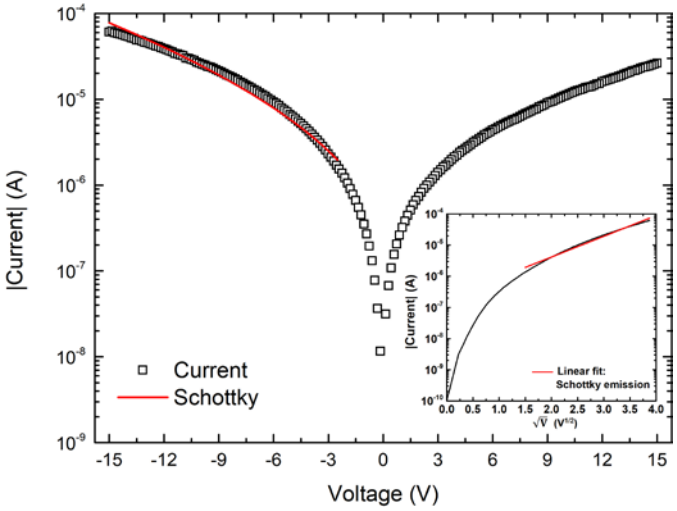

Fig. 6. *I(V) curves of the device and Schottky conduction mechanism fitting.*

ions.

The 650-nm emission band is hidden by the second order resonance of the exciting source, and thus it cannot be quantified correctly. The main peak located at 615 nm falls in the red region of spectrum, and the other two peaks (579 and 591 nm) are in the yellow. An additional peak due to the $^5D_0 \rightarrow {}^7F_4$ transition that should appear at 595 nm was not correctly recorded, because it is close to the limit of the sensitive region of the employed setup configuration. As in the case of Tb^{3+}, the main emission band also presents a double peak feature due to the Stark splitting.

These results evidence that the employed deposition technique and methodology, that takes advantage of the nanomultilayered deposition of different materials, produce optically active RE species, emitting in either the green or red spectral regions, when using Tb or Eu ions, respectively.

C. Electrical characterization

An electroluminescent device is presented in this Master Thesis, composed of Al/Tb/Al/SiO_2. The electrical properties of the fabricated device were analyzed by acquiring the *I*(*V*) curves, grounding the Al bottom electrode with the chuck whereas the ITO contact on top was swept in two regimes: accumulation (negative bias) and inversion (positive bias). The obtained curves for each regime are depicted in Fig. 6. The devices can reach intensities in the order of 10^2 μA, corresponding to -15 V applied. Higher voltages applied were not sustained by the ITO contacts as the current increased to mA.

The curves show an almost symmetric behavior for both regimes, indicating non-rectifying characteristics. The accumulation of charges at the interface with the substrate in the inversion regime creates a barrier that further reduces the charge transport, thus the current is lowered. This could be potentially beneficial to obtain a regulation of EL intensity just by changing the polarity, or in a different sense to employ the device with intermittent emission; but further study is required to determine if this could be possible.

As shown by structural characterization, the device is composed of layers of SiO_2 and Al_2O_3 and thus an insulating behavior is expected, i.e., limited movement of charges. Considering the different conduction mechanisms in dielectric materials, we have assessed the electrical conduction of our devices. We found that the best agreement to the experimental data was obtained when considering an electrode-limited conduction mechanism based on Schottky emission. Thermionic emission of electrons is achieved when a potential barrier formed at a metal-insulator (or semiconductor-insulator) interface is overcome. Applying an external electric field, the barrier can be lowered, easing the emission. This process can be modelled as:

$$J_{\text{Schottky}} = \frac{4\pi m^* q}{h^3} k_B^2 T^2 \exp\left(-\frac{\varphi_B}{k_B T}\right) \exp\left(\frac{\beta}{k_B T} E^{1/2}\right), \quad (1)$$

where φ_B is the potential barrier height in (eV), q the elementary charge, E the applied electric field, k_BT the thermal energy, h the Plank's constant, m^* the effective mass of electrons, and

$$\beta = \sqrt{\frac{q^3}{4\pi\varepsilon_0\varepsilon_r}}, \quad (2)$$

where ε_0 and ε_r are the absolute and relative permittivity respectively [23].

The fitting of the experimental *I*(*V*) data to a Schottky emission model is shown in the inset of Fig. 6, and the result of the fitting to the experimental data is displayed too. It yields a relative dielectric constant of the dielectric layer of ε_r = 18.86, comparable to that of SiO_2 and Al_2O_3 (3.9 and 10.4, respectively).

D. Electroluminescence

Through the application of an electrical current to the device, the Tb^{3+} ions could also be excited to latter emit the excess of energy in the form of light. The integrated total light collected by the PMT is shown in Fig. 7(a) and Fig. 7(b) as a function of the applied voltage and current circulating through the device, respectively. Light emission of enough intensity to be detected by the PMT needs a minimum voltage of 8.5 V. Higher voltages produce an almost exponential increase of the integrated EL.

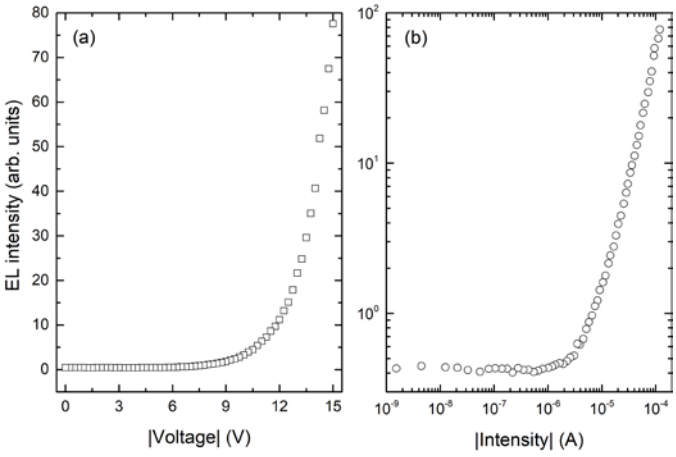

Fig. 7. *Integrated emission of Al/Tb/Al/SiO_2 structure. Data represented is the absolute value of values obtained in accumulation.*

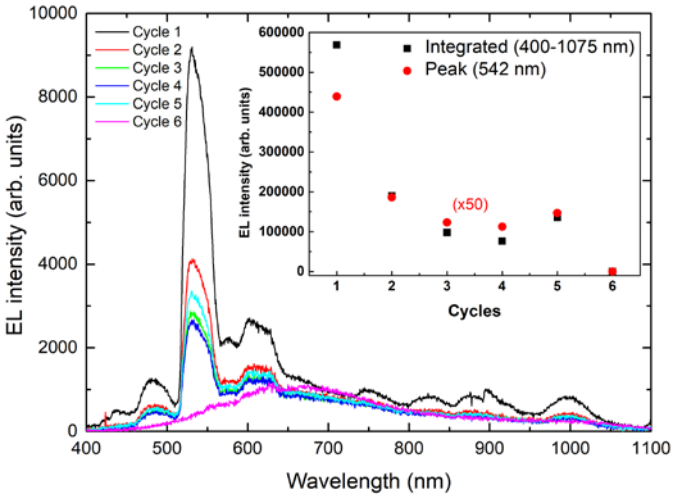

Fig. 8. *EL spectrum of the device for different cycles of 100 µA and 30 s. Inset shows the intensity decay for the complete spectrum (black) and for the main peak of 542 nm (red), corrected with the background of cycle 6.*

Looking at the behavior of the EL with the injected current, we observe a threshold current for emission at ≈ 2 µA, and it increases linearly with the current, which establishes a direct relation between impinging electrons and resulting emitted photons.

On the other hand, Fig. 8 shows the spectrum of light emitted by the device when acquiring the signal for 30 seconds cycles while applying -100 µA at -18 V, in the range of 400-1100 nm. Measured in the first cycle, Tb^{3+} emission bands are located at 483, 531, 576 and 608 nm ($^5D_4 \rightarrow {}^7F_J$, with J = 6, 5, 4 and 3); as well as a blue band located at 437 nm ($^5D_3 \rightarrow {}^7F_4$). These are in good agreement to PL and CL measurements (see Fig. 3), although green bands appear to be slightly shifted from those determined by the electronic transitions previously mentioned. Cycle 6 in the graph shows only the background light emitted by the matrix of the device, and additional peaks at longer wavelengths (≈ 825, 900, 1000 nm) are probably originated in the deep defects in either the SiO_2 or the ITO contact. The inset in the figure displays the decay in intensity both for the 542 nm peak and for the overall of the spectrum, corrected by subtracting the background.

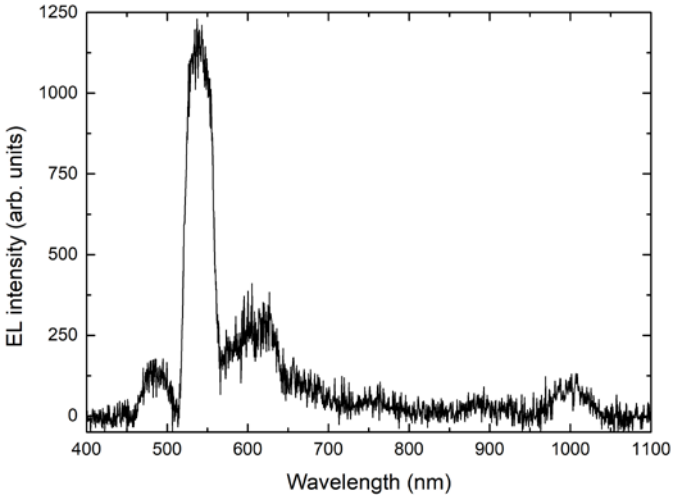

Fig. 9. *EL spectrum of the device under pulsed voltage of 2 V and -8 V applied at 100Hz for a total of 30 s.*

In order to increase the number of cycles with Tb emission, a third EL study was performed by applying pulsed cycles of voltages to the device. It was found that applying 2 V and -8 V at 100 Hz, an EL emission could also be obtained after 30 seconds of acquirement, as shown in Fig 9. In this case only green bands of the Tb^{3+} ions emission can be observed, located at 486, 536, 600 and 623 nm. Further studies are required to determine if pulsed excitation has a lower impact to the oxidation state of Tb atoms than continuous excitation.

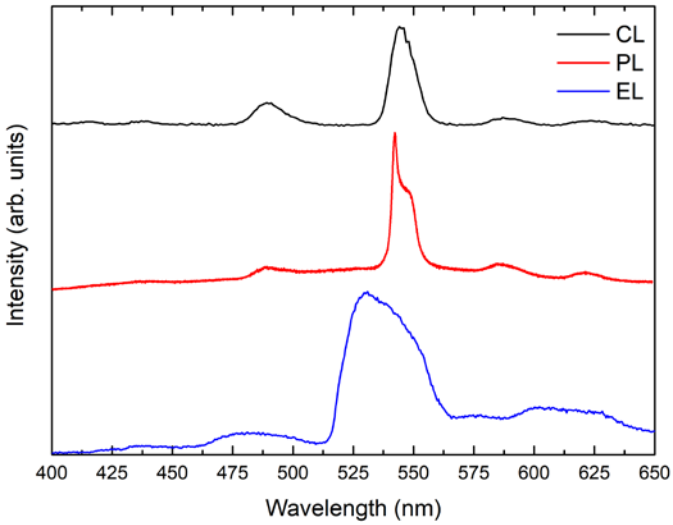

Fig. 10. *Normalized CL, PL (λ_{exc} = 325 nm) and EL emissions of the Al/Tb/SiO_2 structure.*

E. Comparison

All three methods of luminescence, CL, PL (excitation wavelength of 325 nm) and EL, are compared in Fig. 10 for the Al/Tb/Al/SiO_2 sample studied in this project. All three emissions have been normalized for this purpose. As it can be seen, CL spectrum is more intense as the structure, and thus the Tb^{3+} ions, are excited more with this method, meaning also that more emission bands are represented such as those in the blue range. PL emission has the sharpest emission for the principal band of 542 nm. It is evident from the figure that there is a broadening of the EL peaks, which can be attributed to the application of an external electric field during the experiment, which causes the Stark splitting of the bands originally due to the matrix to be magnified.

IV. Discussion

The effect of Al in the Al/Tb/Al/SiO_2 structure has been studied in the works previous to this one (see Ref. 21 and 22). Its presence enhances the optical activation of Tb^{3+} by elimination of bridging between oxygen atoms and formation of Al-O bonds and Tb oxides.

Regarding the conduction mechanisms, we need to keep in mind that the *p*-type Si substrate that is in contact with the Al/RE/Al/SiO_2 layers acts as an electrode, as electrons can travel through all of it. This makes for an electrode-limited conduction mechanism to be the one that best fits the behavior

of electrons, such as Schottky emission (SE) presented before. Others have been tested for the purpose of this project such as Fowler-Nordheim tunneling (FNT) and trap-assisted tunneling (TAT), but they did not fit the experimental data well. As Poole-Frenkel (PF) and space-charge-limited current (SCLC) mechanisms are also frequent in this kind of NML structures they were also tested, being they bulk-limited conduction mechanisms [24]. PF appeared to fit the data very well but the theoretical dielectric constant given was too high ($\varepsilon_r > 300$) and thus was discarded, while SCLC did not yield a good fitting. The presence of Al in the structure is the probable cause for the SE fitting best the data, because electrons must overcome the potential barrier generated by AlO_x layers, as it has been previously reported [25].

Another interesting result is the fact that there is an intensity reduction of the Tb^{3+} EL emission at successive cycles, reaching total quenching of Tb^{3+} emission beyond five cycles (please see spectrum labeled as cycle 6 in Fig. 6, where only the background contribution is observed). This quenching could be related to some atomic structural rearrangement after high electron flux is injected. Indeed, it has been observed in oxide matrices that, under certain excitation conditions, a displacement of oxygen atoms takes place [24], [26]. This, in turn, induces both the creation of alternative (oxygen vacancies-related) conduction paths and the probable reduction of Tb-O bonds, the latter reducing the concentration of optically-active centers. Thus, once these paths are created conduction takes place along nanofilaments with a metallic behavior. This effect has been studied as a possible memory mechanism by creating and destroying these nanofilaments [26]. To avoid their formation and maintain the +3 oxidation state of the Tb ions, an increase of the thermal budget could be beneficial to improve the stability of the Tb_2O_3 phase.

In the case of the structure studied for Eu, Al was not added as Eu is very easily oxidized already (Eu is quickly oxidized when exposed to air). The evaporation during the deposition is then done from a target containing already oxidized Eu and thus its deposition also results in Eu oxide, with Eu^{3+} ions optically active (see spectrum labeled as as-deposit in Fig. 4). This meant that Eu oxides could already be easily obtained without the need of employing Al. PL measurements here presented demonstrated that this is the case as Eu^{3+} ions emission can be very well distinguished. Thus, the presence of Al seems not to be a requirement for good emission. However, future work should be done to study if the incorporation Al supposes a benefit to the sample, either by increasing the oxidation of Eu and thus enhancing the emission of Eu^{3+} ions; or by reducing the background emission.

Both materials here studied demonstrate that sharp emissions of RE species can be obtained, in this case in the green and red regions of the spectrum. Thus, they can be considered potential candidates for future optoelectronics applications, in particular as integrated light emitting devices.

V. Conclusion

$Al/Tb/Al/SiO_2$ nanomultilayers have been fabricated employing electron-beam evaporation by evaporating alternatively layers of each material. It had been previously studied the positive effect of Al in the optical activation of Tb^{3+} ions and the optimal annealing temperature to be applied to the layers. Optical characterization by means of PL and CL showed that Tb^{3+} ions had been optically activated. Electrical characterization allowed inferring that the conduction mechanism governing the structure is due to Schottky emission, although thermal activated mechanisms cannot be discarded. Integrated EL characterized the threshold current and voltage to obtain emission from the devices and the spectrum of this emission confirmed that it corresponded to Tb^{3+}, as well as matrix defect-related emissions. EL spectrum was also obtained with a pulsed voltage signal.

An Eu/SiO_2 NML structure was also fabricated by EBE in this Master Thesis. XPS measurements of this sample showed the presence of Si-rich SiO_2 doped with Eu. PL measurements of the sample concluded that optically active Eu^{3+} ions can be achieved with this structure, optimized for a thermal annealing at 700 °C.

The results presented prove that the combination of electron-beam evaporation and nanomultilayer structures are useful to obtain luminescent $Al/RE/Al/SiO_2$ and RE/SiO_2 systems that can be applied in the field of optoelectronics and lasing.

Acknowledgment

I would like to start by thanking my tutors Dr. Sergi Hernández and MSc. Oriol Blázquez for their support and counseling throughout this year, as well as Prof. Blas Garrido for his additional tips and advices.

I would also like to thank all the friends I have met during this Master, with a desire for the brightest of futures. A special mention goes to Bea for her unconditional support and patience during many of my uninterrupted work hours.

And last, I want to give credit to my family and friends in Vilagarcía de Arousa, as their strength has always kept me going to reach all my goals.

References

[1] "Efficient blue light-emitting diodes leading to bright and energy-saving white light sources", The Nobel Prize in Physics 2014 - Advanced Information, [online], *Nobel Media AB*, Available: http://www.nobelprize.org/nobel_prizes/physics/laureates/2014/advanced.html, 2014; Accessed: 10/06/2017.

[2] K. D. Hirschman, L. Tsybeskov, S. P. Duttagupta and P. Fauchet, "Silicon-based visible light-emitting devices integrated into microelectronic circuits," *Nature*, vol. 384, no. 6607, p. 338, November 1996.

[3] G. T. Reed, G. Mashanovich, F. Y. Gardes and D. J. Thomson, "Silicon optical modulators," *Nature photonics*, vol. 4, no. 8, pp. 518-526, July 2010.

[4] D. J. Miller, P. M. Watts and A. W. Moore, "Motivating future interconnects: a differential measurement analysis of PCI latency," *Proceedings of the 5th ACM/IEEE Symposium on Architectures for Networking and Communications Systems*, ACM, pp. 94-103, 2009.

[5] S. Yerci, R. Li, and L. Dal Negro, "Electroluminescence from Er-doped Si-rich silicon nitride light emitting diodes," *Applied Physics Letters*, vol. 97, no. 8, p. 081109, August 2010.

[6] A. J. Kenyon, "Recent developments in rare-earth doped materials for optoelectronics," *Progress in Quantum Electronics*, vol. 26, no. 4, pp. 225-284, October 2002.

[7] Shibin Jiang (Ed.), *Proceedings of the SPIE VII Conference on Rare-Earth Doped Materials and Devices*, vol 4990, June 2003.

[8] J. Li, O. H. Zalloum, T. Roschuk, C. L. Heng, J. Wojcik and P. Mascher, "Light emission from rare-earth doped silicon nanostructures," *Advances in Optical Technologies*, March 2008.

[9] A. J. Kenyon, P. F. Trwoga, M. Federighi and C. W. Pitt, "Optical properties of PECVD erbium-doped silicon-rich silica: evidence for energy transfer between silicon microclusters and erbium ions," *Journal of Physics: Condensed Matter*, vol. 6, no. 21, L319-L324, March 1994.

[10] J. M. Ramírez, Y. Berencén, L. López-Conesa, J. M. Rebled, F. Peiró and B. Garrido, "Carrier transport and electroluminescence efficiency of erbium-doped silicon nanocrystal superlattices," *Applied Physics Letters*, vol. 103, no. 8, p. 081102, August 2013.

[11] Y. Berencén et al., "Intense green-yellow electroluminescence from Tb+-implanted silicon-rich silicon nitride/oxide light emitting devices," *Applied Physics Letters*, vol. 103, no. 11, p. 111102, September 2013.

[12] S. Boninelli, G. Bellocchi, G. Franzò, M. Miritello and F. Iacona, "New strategies to improve the luminescence efficiency of Eu ions embedded in Si-based matrices," *Journal of Applied Physics*, vol. 113, no. 14, p. 143503, April 2013.

[13] A. J. Silversmith, D. M. Boye, K. S. Brewer, C. E. Gillespie, Y. Lu, and D. L. Campbell, "5 D 3→ 7 F J emission in terbium-doped sol–gel glasses," *Journal of luminescence*, vol. 121, no. 1, pp. 14-20, November 2006.

[14] C. B. De Araujo, D. Silvério da Silva, T. A. Alves de Assumpção, L. R. P. Kassab, and D. Mariano da Silva, "Enhanced optical properties of germanate and tellurite glasses containing metal or semiconductor nanoparticles," *The Scientific World Journal*, vol. 2013, Article ID 385193, January 2013.

[15] P. Ruterana, M. P. Chauvat and K. Lorenz, "Rare earth ion implantation and optical activation in nitride semiconductors for multicolor emission," *Semiconductor Science and Technology*, vol. 30, no. 4, p. 044004, March 2015.

[16] J. L. Deschanvres, W. Meffre, J. C. Joubert, J. P. Senateur, F. Robaut, J. E. Broquin and R. Rimet, "Rare earth-doped alumina thin films deposited by liquid source CVD processes," *Journal of alloys and compounds*, vol. 275, pp. 742-745, September 1998.

[17] T. Minami, T. Yamamoto and T. Miyata, "Highly transparent and conductive rare earth-doped ZnO thin films prepared by magnetron sputtering," *Thin Solid Films*, vol. 366, no. 1, pp. 63-68, January 2000.

[18] X. P. Zhao and J. B. Yin, "Preparation and electrorheological characteristics of rare-earth-doped TiO2 suspensions," *Chemistry of Materials*, vol. 14, no. 5, pp. 2258-2263, February 2002.

[19] L. Norin, E. Vanin, P. Soininen and M. Putkonen, "Atomic layer deposition as a new method for rare-earth doping of optical fibers" in *Conference on Lasers and Electro-Optics*, Optical Society of America, May 2007.

[20] O. Blázquez, J. M. Ramírez, J. López-Vidrier, Y. Berencén, S. Hernández, P. Sanchis and B. Garrido, "Luminescence yield in Al and Tb3+ delta-doped oxide thin films fabricated by electron beam evaporation," in *SPIE Microtechnologies*, pp. 95200K-95200K, International Society for Optics and Photonics, June 2015.

[21] O. Blázquez et al., "Structural and optical properties of Al-Tb/SiO2 multilayers fabricated by electron beam evaporation," *Journal of Applied Physics*, vol. 120, no. 13, p. 135302, October 2016.

[22] H. S. Ahmed, O. M. Ntwaeaborwa, M. A. Gusowski, J. R. Botha, and R. E. Kroon, "5 D 3→ 7 F J emission of Tb doped sol–gel silica," *Physica B: Condensed Matter*, vol. 407, no. 10, pp. 1653-1655, May 2012.

[23] J. M. Ramírez, "Rare Earth-Doped Silicon-Based Light Emmiting Devices: Towards new Integrated Photonic Building Blocks," Ph.D. thesis, Dept. d'Electrònica, University de Barcelona, Barcelona, Spain, June 2015.

[24] E. W. Lim, and R. Ismail, "Conduction mechanism of valence change resistive switching memory: a survey," *Electronics*, vol. 4, no. 3, pp. 586-613, September 2015.

[25] C. J. Li, S. Jou, and W. L. Chen, "Effect of Pt and Al electrodes on resistive switching properties of sputter-deposited Cu-doped SiO2 Film," *Japanese Journal of Applied Physics*, vol. 50, no. 1S2, p. 01BG08, January 2011.

[26] I. Valov, "Redox-Based Resistive Switching Memories (ReRAMs): Electrochemical Systems at the Atomic Scale," *ChemElectroChem*, vol. 1, no. 1, pp. 26-36, January 2014.